

## Solid-State NMR Reveals Structural and Dynamical Properties of a Membrane-Anchored Electron-Carrier Protein, Cytochrome *b*<sub>5</sub>

Ulrich H. N. Dürr,<sup>†</sup> Kazutoshi Yamamoto,<sup>†</sup> Sang-Choul Im,<sup>‡</sup> Lucy Waskell,<sup>‡</sup> and Ayyalusamy Ramamoorthy<sup>\*†</sup>

Biophysics Research Division and Department of Chemistry, University of Michigan, Ann Arbor, Michigan 48109-1055, and Department of Anesthesiology, University of Michigan, and VA Medical Center, Ann Arbor, Michigan 48105

Received December 17, 2006; E-mail: ramamoor@umich.edu

The vast majority of pharmaceutical compounds in use today are hydrophobic compounds. The human metabolism oxidizes them to water-soluble, excretable compounds by a superfamily of enzymes known as the cytochromes P450 (cyt P450).<sup>1</sup> These enzymes are sometimes referred to as “Mother Nature’s blowtorch” because they are such strong and versatile oxidizing agents. Cytochrome *b*<sub>5</sub> (cyt *b*<sub>5</sub>) is a membrane-bound protein which enhances the efficiency of the metabolism of selected drugs by cyt P450, by donating an electron to cyt P450.<sup>2,3</sup> Besides augmenting drug metabolism, cyt *b*<sub>5</sub> is also essential for the biosynthesis of testosterone and numerous unsaturated lipids which are necessary for maintaining the integrity of cellular membranes.<sup>3</sup> In order to understand the molecular mechanism by which cyt *b*<sub>5</sub> increases the efficiency of oxidation by cyt P450 in vivo, one must understand the structural folding of cyt *b*<sub>5</sub> that enables it to interact with cyt P450.

Full-length rabbit cyt *b*<sub>5</sub> is a 16.7 kDa protein consisting of three domains: a 95 amino acid amino terminal heme-containing domain, a 25 amino acid carboxyl terminal membrane anchor domain, and a 14 amino acid linker region which connects the former two.<sup>3,4</sup> Figure 1A shows a model constructed from the solution NMR structure of the soluble domain of rabbit cyt *b*<sub>5</sub>;<sup>5</sup> the full amino acid sequence is given as Supporting Information. Because of the difficulties in preparing suitable samples of full-length cyt *b*<sub>5</sub>, X-ray<sup>6</sup> and solution NMR<sup>3,7</sup> studies reported the structure of the water-soluble domain of cyt *b*<sub>5</sub> that lacks the transmembrane domain. Remarkably, the soluble domain alone is not able to fulfill its physiological functions.<sup>3,8</sup> Hence, it is vital to investigate the role of the membrane-bound domain and the linker region in the function of cyt *b*<sub>5</sub> in order to fully understand the interaction with cyt P450. A determination of the three-dimensional structure, dynamics, and the relative orientation of these domains in a membrane environment will shed light on how cyt *b*<sub>5</sub> carries out its function. Here, we report the first solid-state NMR investigation of the membrane topology and related dynamic properties of full-length rabbit cyt *b*<sub>5</sub> in a membrane environment.

Lipid bicelles<sup>9</sup> were prepared from dimyristoylphosphatidylcholine (DMPC) and dihexanoylphosphatidylcholine (DHPC) in a 3.5:1 molar ratio; cyt *b*<sub>5</sub> was added in different amounts as described in the Supporting Information. The bicelle samples were magnetically aligned with the bilayer normal perpendicular to the external magnetic field for solid-state NMR experiments. The quality and extent of magnetic alignment of the bicelles containing various concentrations of cyt *b*<sub>5</sub> were examined using <sup>31</sup>P chemical shift spectra of samples (representative spectra are given as Supporting Information). Bicelles containing high concentrations (>0.5 mol %) of protein did not align well, while they did align well upon lowering the protein concentration and are suitable for solid-state NMR stud-

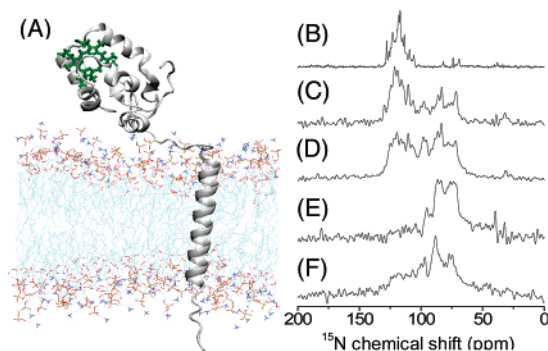


**Figure 1.** Molecular model and <sup>15</sup>N NMR spectra of uniformly aligned DMPC:DHPC bicelles containing <sup>15</sup>N-labeled cyt *b*<sub>5</sub>. The model (A) shows cyt *b*<sub>5</sub> in the context of a DMPC bilayer; the transmembrane, linker, and heme-carrying soluble domains are evident. The <sup>15</sup>N RINEPT spectrum (B) shows spectral intensity only in the 100–130 ppm region, consistent with a high mobility of the soluble domain. In the RINEPT sequence, 2.6 and 1.3 ms were used in the first (before the pair of 90° pulses) and second (after the pair of 90° pulses) delays, respectively. This spectral region (100–130 ppm) also shows peaks in cross-polarization (CP) spectra at 3.0 ms (C) and 0.8 ms (D) contact times. At a short contact time of 0.1 ms (E), however, spectral intensity is mostly observed in the range from 40 to 90 ppm. This spectral component is most likely from the relatively immobile transmembrane domain. A D<sub>2</sub>O exchange experiment (F) with a 0.8 ms contact time confirms this spectral assignment.

ies. At the end of the experiments, the <sup>15</sup>N NMR spectra and the molecular weight of cyt *b*<sub>5</sub> were checked to rule out protein degradation.

<sup>15</sup>N chemical shift spectra of uniformly <sup>15</sup>N-labeled cyt *b*<sub>5</sub> in aligned DMPC:DHPC bicelles show a strong dependence of the spectral line shape on experimental conditions (Figure 1). The <sup>15</sup>N cross-polarization (CP) spectrum obtained at 0.8 ms contact time (Figure 1D) displays the strongest overall intensity and most likely contains signal from the entire protein. It may be expected that the transmembrane (TM) domain of cyt *b*<sub>5</sub> is relatively more rigid on the NMR time scale, while the water-soluble domain is less rigid. Therefore, it should be possible to distinguish resonances from these two regions based on the difference in <sup>15</sup>N–<sup>1</sup>H dipolar coupling values. Indeed, we have obtained markedly different <sup>15</sup>N spectra when the CP contact time was varied to control the extent of magnetization transfer from <sup>1</sup>H to <sup>15</sup>N nuclei (Figure 1C–E). The spectra suggest that a shorter contact time of 0.1 ms is sufficient to transfer magnetization from <sup>1</sup>H to <sup>15</sup>N in the rigid residues as found in the TM domain. These experimental conditions result in resonances in the 40–90 ppm range (Figure 1E). Interestingly, the signal in the 100–130 ppm region is suppressed to a great extent. On the other hand, since a longer contact time transfers magnetization to all parts of the molecule due to <sup>1</sup>H spin diffusion, the spectra at 3 ms (Figure 1C) and 0.8 ms (Figure 1D) contact time contain peaks in the entire <sup>15</sup>N chemical shift frequency range. Hence, we

<sup>†</sup> Biophysics Research Division and Department of Chemistry.

<sup>‡</sup> Department of Anesthesiology and VA Medical Center.

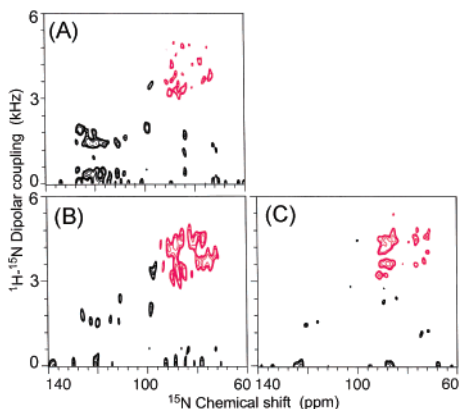


**Figure 2.**  $^{15}\text{N}$ -HIMSELF spectra of  $\text{U-}^{15}\text{N}$ -cyt  $b_5$ , recorded with a CP contact time of 0.8 ms (A) and 0.1 ms (B). (C) Recorded after the water in the bicelle sample was replaced by  $\text{D}_2\text{O}$ , suppressing the spectral contributions of the soluble domain.

presume that the signal appearing between 100 and 130 ppm originates from the less rigid residues in the soluble domain. This supposition is confirmed by a RINEPT (refocused insensitive nuclei enhanced by polarization transfer) experiment<sup>10</sup> shown in Figure 1B. Since no decoupling pulses were employed during the evolution and refocusing delays of the RINEPT sequence, the  $^{15}\text{N}$  transverse magnetization evolves under the motionally averaged  $^1\text{H-}^{15}\text{N}$  and  $^1\text{H-}^1\text{H}$  dipolar and  $^1\text{H-}^{15}\text{N}$  scalar couplings. The time delays in the RINEPT sequence were experimentally optimized to obtain the signal from the less rigid residues found in the soluble domain of the protein. Interestingly, the RINEPT sequence significantly suppressed the peaks from the TM domain that resonate between 40 and 90 ppm. This is mainly because the transverse magnetization from the TM region dephases relatively quickly in the evolution and refocusing periods of the RINEPT sequence due to relatively strong  $^1\text{H-}^{15}\text{N}$  and  $^1\text{H-}^1\text{H}$  dipolar couplings.

Amide protons can be exchanged with deuterons when exposed to  $\text{D}_2\text{O}$ , thus suppressing the  $^{15}\text{N}$  signal from water-exposed protein domains.<sup>11</sup> This approach was utilized to suppress amide  $^{15}\text{N}$  signals from the cyt  $b_5$   $^{15}\text{N}$  spectrum. The  $^{15}\text{N}$  CP spectrum of bicelles, where water was exchanged with  $\text{D}_2\text{O}$ , is given in Figure 1F. It contains peaks from the TM region (40–90 ppm) but not from the soluble domain (100–130 ppm) of the protein, again supporting our assignment. These 1D spectral editing approaches demonstrate that the dynamics of the transmembrane and soluble domains are very different and that it is possible to differentiate between the resonances from these domains, which is highly valuable to interpret data from PISEMA<sup>12</sup> (polarization inversion and spin exchange at the magic angle)-type experiments in terms of structure and geometry of cyt  $b_5$ .

Two-dimensional separated local field spectra, which correlate  $^{15}\text{N}$  chemical shift with  $^1\text{H-}^{15}\text{N}$  dipolar coupling, were recorded on well-oriented bicelles and are given in Figure 2. A HIMSELF<sup>13</sup> (heteronuclear isotropic mixing leading to spin exchange via the local field) sequence based on the PIWIMz (polarization inversion by windowless isotropic mixing) pulse scheme was used, which we recently found to give better resolution when compared to the more commonly employed PISEMA sequence.<sup>12</sup> Figure 2A shows that the 1D spectral region assigned to the TM anchor region of the protein assumes a distinct circular PISA (polarity index slant angle)-wheel pattern<sup>14</sup> when expanded into the second dimension of  $^1\text{H-}^{15}\text{N}$  dipolar coupling, indicative of  $\alpha$ -helical conformation. Spectrum 2A also proves that the signal from the soluble domain, although resonating in the 100–130 ppm region characteristic for isotropic  $^{15}\text{N}$  chemical shifts, shows clearly resolved residual  $^1\text{H-}$

$^{15}\text{N}$  dipolar couplings. This suggests that the soluble domain is weakly aligned. When performed in combination with the above-mentioned spectral editing techniques, the 2D HIMSELF experiments demonstrate that it is possible to obtain the resonances from the transmembrane helical region alone by suppressing most other resonances from cyt  $b_5$  (Figure 2B,C).

Spectral simulations were carried out to infer the tilt of the TM  $\alpha$ -helix from the observed PISA wheel. The dispersion of resonances in the PISA wheel is consistent with a  $15(\pm 3)^\circ$  tilt of the TM helix relative to the bilayer normal. However, no single PISA wheel could give a satisfactory fit to all resonances present in the circular pattern, indicating that the helical TM domain may not be a perfect  $\alpha$ -helix. The Pro-116 residue located in the middle of the TM region could induce a kink in the helical structure, which may be responsible for this observation of an imperfect PISA wheel. Further experimental studies are in progress to completely assign the spectrum.

In this study, we have presented a first structural study on holo-cyt  $b_5$  in a membrane environment. We found an  $\alpha$ -helical structure for the rigid transmembrane region, with untypical geometrical imperfection due to the Pro residue, and very fast dynamics for the soluble domain. We believe that the presented results point out a versatile way to investigate numerous structural and dynamic properties of cyt  $b_5$  and its physiologically important interaction with cyt P450. The successful demonstration of spectral editing approaches will significantly reduce the difficulties in the resonance assignment of cyt  $b_5$ . Moreover, the combination of these unique NMR spectral editing methods will be applicable in the structural and dynamical studies of a large number of other membrane proteins, as well.

**Acknowledgment.** This study was supported by research funds from NIH (AI054515 to A.R. and GM035533 to L.W.) and a VA Merit Review grant to L.W.

**Supporting Information Available:** Sequence of cyt  $b_5$ , protein expression protocol, bicelle preparation protocol, and  $^{31}\text{P}$  spectra of bicelles, HIMSELF and PISEMA spectra, and best-fit simulations. This material is available free of charge via the Internet at <http://pubs.acs.org>.

## References

- (1) (a) Denisov, I. G.; Makris, T. M.; Sligar, S. G.; Schlichting, I. *Chem. Rev.* **2005**, *105*, 2253. (b) Guengerich, F. P. *Mechanism and Biochemistry*, 3rd ed.; de Montellano, P. O., Ed.; Plenum Publishers: New York, 2005.
- (2) Zhang, H.; Myshkin, E.; Waskell, L. *Biochem. Biophys. Res. Commun.* **2005**, *338*, 499.
- (3) (a) Vergères, G.; Waskell, L. *Biochimie* **1995**, *77*, 604. (b) Schenkman, J. B.; Jansson, I. *Pharmacol. Ther.* **2003**, *97*, 139.
- (4) Mulrooney, S. B.; Waskell, L. *Protein Expr. Purif.* **2000**, *19*, 173.
- (5) Banci, L.; Bertini, I.; Rosato, A.; Scacchieri, S. *Eur. J. Biochem.* **2000**, *267*, 755.
- (6) Durlley, R. C. E.; Mathews, F. S. *Acta Crystallogr.* **1996**, *D52*, 65.
- (7) (a) Guiles, R. D.; Basus, V. J.; Kuntz, I. D.; Waskell, L. *Biochemistry* **1992**, *31*, 11365. (b) Muskett, F. W.; Kelly, G. P.; Whitford, D. J. *Mol. Biol.* **1996**, *258*, 172.
- (8) Clarke, T. A.; Im, S.-C.; Bidwai, A.; Waskell, L. *J. Biol. Chem.* **2004**, *279*, 36809.
- (9) (a) Sanders, C. R.; Prestegard, J. H. *Biophys. J.* **1990**, *58*, 447. (b) Sanders, C. R.; Hare, B. J.; Howard, K. P.; Prestegard, J. H. *Prog. Nucl. Magn. Reson. Spectrosc.* **1994**, *26*, 421. (c) Prosser, R. S.; Evancics, F.; Kiteviski, J. L.; Al-Abdul-Wahid, M. S. *Biochemistry* **2006**, *45*, 8453. (d) Lu, J. X.; Damodaran, K.; Lorigan, G. A. *J. Magn. Reson.* **2006**, *178*, 283–287.
- (10) Burum, D. P.; Ernst, R. R. *J. Magn. Reson.* **1980**, *39*, 163.
- (11) Li, R.; Woodward, C. *Protein Sci.* **1999**, *8*, 1571.
- (12) (a) Wu, C. H.; Ramamoorthy, A.; Opella, S. J. *J. Magn. Reson., Ser. A* **1994**, *109*, 270. (b) Ramamoorthy, A.; Wei, Y.; Lee, D. K. *Annu. Rep. NMR Spectrosc.* **2004**, *52*, 1–52. (c) Yamamoto, K.; Lee, D. K.; Ramamoorthy, A. *Chem. Phys. Lett.* **2005**, *407*, 289–293.
- (13) (a) Dvinskikh, S. V.; Yamamoto, K.; Ramamoorthy, A. *J. Chem. Phys.* **2006**, *125*, 34507. (b) Dvinskikh, S.; Dürr, U.; Yamamoto, K.; Ramamoorthy, A. *J. Am. Chem. Soc.* **2006**, *128*, 6326–6327.
- (14) (a) Marassi, F. M.; Opella, S. J. *J. Magn. Reson.* **2000**, *144*, 150. (b) Denny, J. K.; Wang, J.; Cross, T. A.; Quine, J. R. *J. Magn. Reson.* **2001**, *152*, 217.

JA069028M